Andersen's syndrome mutants produce a knockdown of inwardly rectifying K+ channel in mouse skeletal muscle in vivo

Dina Simkin, Gaëlle Robin, Serena Giuliano, Ana Vukolic, Pamela Moceri, Nicolas Guy, Kay-Dietrich Wagner, Alain Lacampagne, Bruno Allard, Saïd Bendahhou

Andersen's syndrome mutants produce a knockdown of inwardly rectifying K^+ channel in mouse skeletal muscle in vivo

Dina Simkin[1,2] · **Gaëlle Robin**[3] · **Serena Giuliano**[1] · **Ana Vukolic**[4] · **Pamela Moceri**[1,5] · **Nicolas Guy**[6] · **Kay-Dietrich Wagner**[7] · **Alain Lacampagne**[8] · **Bruno Allard**[3] · **Saïd Bendahhou**[1]

Abstract Andersen's syndrome (AS) is a rare autosomal disorder that has been defined by the triad of periodic paralysis, cardiac arrhythmia, and developmental anomalies. AS has been directly linked to over 40 different autosomal dominant negative loss-of-function mutations in the *KCNJ2* gene, encoding for the tetrameric strong inward rectifying K^+ channel $K_{IR}2.1$. While $K_{IR}2.1$ channels have been suggested to contribute to setting the resting membrane potential (RMP) and to control the duration of the action potential (AP) in skeletal and cardiac muscle, the mechanism by which AS mutations produce such complex pathophysiological symptoms is poorly understood. Thus, we use an adenoviral transduction strategy to study in vivo subcellular distribution of wild-type (WT) and AS-associated mutant $K_{IR}2.1$ channels in mouse skeletal muscle. We determined that WT and D71V AS mutant $K_{IR}2.1$ channels are localized to the sarcolemma and the transverse tubules (T-tubules) of skeletal muscle fibers, while the Δ314-315 AS $K_{IR}2.1$ mutation prevents proper trafficking of the homo- or hetero-meric channel complexes. Whole-cell voltage-clamp recordings in individual skeletal muscle fibers confirmed the reduction of inwardly rectifying K^+ current (I_{K1}) after transduction with Δ314-315 $K_{IR}2.1$ as compared to WT channels. Analysis of skeletal muscle function revealed reduced force generation during isometric contraction as well as reduced resistance to muscle fatigue in *extensor digitorum longus* muscles transduced with AS mutant $K_{IR}2.1$. Together, these results suggest that $K_{IR}2.1$ channels may be involved in the excitation–contraction coupling process required for proper skeletal muscle function. Our findings provide clues to mechanisms associated with periodic paralysis in AS.

Keywords Andersen's syndrome · $K_{IR}2.1$ · Skeletal muscle · Adenovirus · Channelopathies

✉ Saïd Bendahhou
said.bendahhou@unice.fr

[1] UMR 7370 CNRS, LP2M, Laboratoire d'Excellence - ICST, Université Côte d'Azur, Faculté de Médecine, 06107 Nice, France

[2] Department of Pharmacology, Feinberg School of Medicine, Northwestern University, Chicago, IL 60611, USA

[3] UMR CNRS 5534, Université Claude Bernard Lyon 1, 69622 Lyon, France

[4] Institute for Molecular Health Science, ETH Zurich, 8093 Zurich, Switzerland

[5] Service de Cardiologie, Pasteur Hospital, CHU de Nice, 06107 Nice, France

[6] UMR 7275 CNRS, IPMC, Université Côte d'Azur, 06560 Valbonne, France

[7] UMR 7284 CNRS, INSERM, IBV, Université Côte d'Azur, Faculté de Médecine, 06107 Nice, France

[8] INSERM U1046, UMR CNRS 9214, Université de Montpellier, CHRU de Montpellier, 34295 Montpellier, France

Introduction

Andersen's syndrome (AS) is a multi-organ disorder presenting with periodic paralysis, cardiac arrhythmias and developmental abnormalities, (Andersen et al. 1971) including bone malformation and cognitive anomalies (Yoon et al. 2006). Mutations of the *KCNJ2* gene (which encodes the inward rectifier K^+ channel $K_{IR}2.1$) were found through genomic DNA screening of AS patients (Plaster et al. 2001). In addition, a mutation on the *KCNJ5* gene (encoding $K_{IR}3.4$ channel) has recently been reported to be associated with AS clinical phenotype, by an inhibitory modulation of $K_{IR}2.1$ (Kokunai et al. 2014). In vitro and ex vivo studies have shown

that most AS-associated mutations cause a dominant negative suppression of $K_{IR}2.1$ channel function leading to silent channels (Bendahhou et al. 2003; Miake et al. 2003; Plaster et al. 2001; Priori et al. 2005; Sacconi et al. 2009; Tristani-Firouzi et al. 2002). Studies on $K_{IR}2.1$ and AS-associated $K_{IR}2.1$ mutant channels in cardiac muscle have provided much evidence supporting a role of these channels in resting membrane potential (RMP) regulation and the duration of the late repolarization phase of the cardiac action potential (Miake et al. 2003). In ventricular myocytes, the inward rectifier current (I_{K1}) is essential in the regulation of action potential repolarization and stabilization of the resting membrane potential (Lopatin and Nichols 2001; Miake et al. 2003). However, the role of $K_{IR}2.1$ in skeletal muscle and the molecular basis by which loss of $K_{IR}2.1$ function causes periodic paralysis has not yet been established.

In skeletal muscle, the $K_{IR}2.1$ K^+ channel is the key inwardly rectifying channel thought to be involved in setting the RMP, regulating electrical excitability and clearance of K^+ from the T-tubule system (Hibino et al. 2010; Kristensen et al. 2006; Sacco et al. 2014; Sacconi et al. 2009). The abundant distribution of $K_{IR}2.1$ channels in skeletal muscle is imperative to proper function (Doupnik et al. 1995). Moreover, similarities between AS and other skeletal muscle disorders may provide some clues about other molecular mechanisms that may be relevant in AS. For instance, two-thirds of AS patients exhibit hypokalemic periodic paralysis, a primary symptom of Na^+ or Ca^{2+} channel mutations (Tristani-Firouzi et al. 2002). Calcium channel mutations cause hypokalemic periodic paralysis by disturbing excitation–contraction coupling, which is important for generation of muscle contraction and contractile strength (Fontaine et al. 1994).

The inward rectifier potassium channel (K_{IR}) family is subdivided into seven members according to amino acid sequence homology (Doupnik et al. 1995). The K_{IR} subunit is formed by two membrane-spanning segments, namely M1 and M2, a pore-forming loop between the two transmembrane segments and amino and carboxyl *termini* located intracellularly. Four subunits co-assemble in a homo- or heterotetrameric manner to form a functional channel (Yang et al. 1995). *KCNJ* genes are widely expressed in the body. They can be found in muscle (*KCNJ2*, *KCNJ11*, *KCNJ18*), heart (*KCNJ2*, *KCNJ3*, *KCNJ5*, *KCNJ11*), brain (*KCNJ3*, *KCNJ6*, *KCNJ9*, *KCNJ11*), epithelial (*KCNJ1*, *KCNJ2*) and many other tissues (Inagaki et al. 1995; Lesage et al. 1995; Raab-Graham et al. 1994; Ryan et al. 2010; Sakura et al. 1995a, b; Stoffel et al. 1994; Tucker et al. 1995; Yano et al. 1994). The K_{IR} channel family shares not only a common structural motif but also a high primary structure similarity. $K_{IR}2.1$ channels have been shown to be localized in the sarcolemma membranes and T-tubules of skeletal and heart muscles through the use of polyclonal antibodies (Ashcroft et al. 1985; Christe 1999; Clark et al. 2001; Vaidyanathan et al. 2010). However, these antibodies have not been tested for their specificity or, especially, for their capability to discriminate between K_{IR} channel isoforms that are expressed in the same tissue. Moreover, localization of AS-associated mutations in vivo has not been performed. As skeletal and heart muscles have complex structures and compartments, precise localization of $K_{IR}2.1$ channels within these tissues can contribute to our understanding of the muscle molecular architecture and ultimately to the involvement of these channels in AS pathophysiology and other skeletal- and cardiac muscle-related pathologies. We developed an adenovirus (Ad)-induced animal model, overexpressing $K_{IR}2.1$ and/or AS-associated mutations in order to evaluate the localization of these channels in skeletal muscle subcellular compartments. We also evaluated the consequences of overexpressing AS $K_{IR}2.1$ mutants using voltage-clamp analysis in single mouse skeletal muscle fibers as well as the contractility and fatigability of these skeletal muscles.

Expanding our research field to in vivo will help to better define the role of I_{k1} currents in skeletal muscle and may facilitate the development of gene or drug therapies to better treat periodic paralyzes associated with $K_{IR}2.1$ channelopathy.

Methods

Adenovirus strategy

The full-length coding sequence of human $K_{IR}2.1$ (Ashen et al. 1995) was cloned into a pDNR-expressing vector with EcoR1 and Xho1 restriction enzyme sites and under the control of the CMV promoter. Each construct was made with wild-type (WT) or a typical AS mutant $K_{IR}2.1$ channel sequence (Bendahhou et al. 2003) and used in adenovirus type-5 production (Atlantic Gene Therapies Platform; Nantes, France) (Graham et al. 1989). We chose two representative AS mutations, D71V (silent channels at the cell surface) and Δ314-315 (mistrafficking), for study (Fig. 1a). These constructs were made with either a fused EGFP or a HA tag (Fig. 1a) for detection: Ad-WT-HA, Ad-WT-EGFP, Ad-D71V-EGFP, Ad-D71V-HA, Ad-Δ314-315-EGFP and Ad-Δ314-315-HA.

Cell culture

COS-7 cells were maintained in Dulbecco's modified Eagle medium supplemented with 10% fetal bovine serum and 100 U/mL streptomycin, 100 U/mL penicillin, at 37 °C in a humidified 5% CO_2 atmosphere. COS-7 cells were transduced with 2 adenovirus particles per cell carrying $K_{IR}2.1$-EGFP in 35-mm culture dishes. Currents were recorded 24 h after induction.

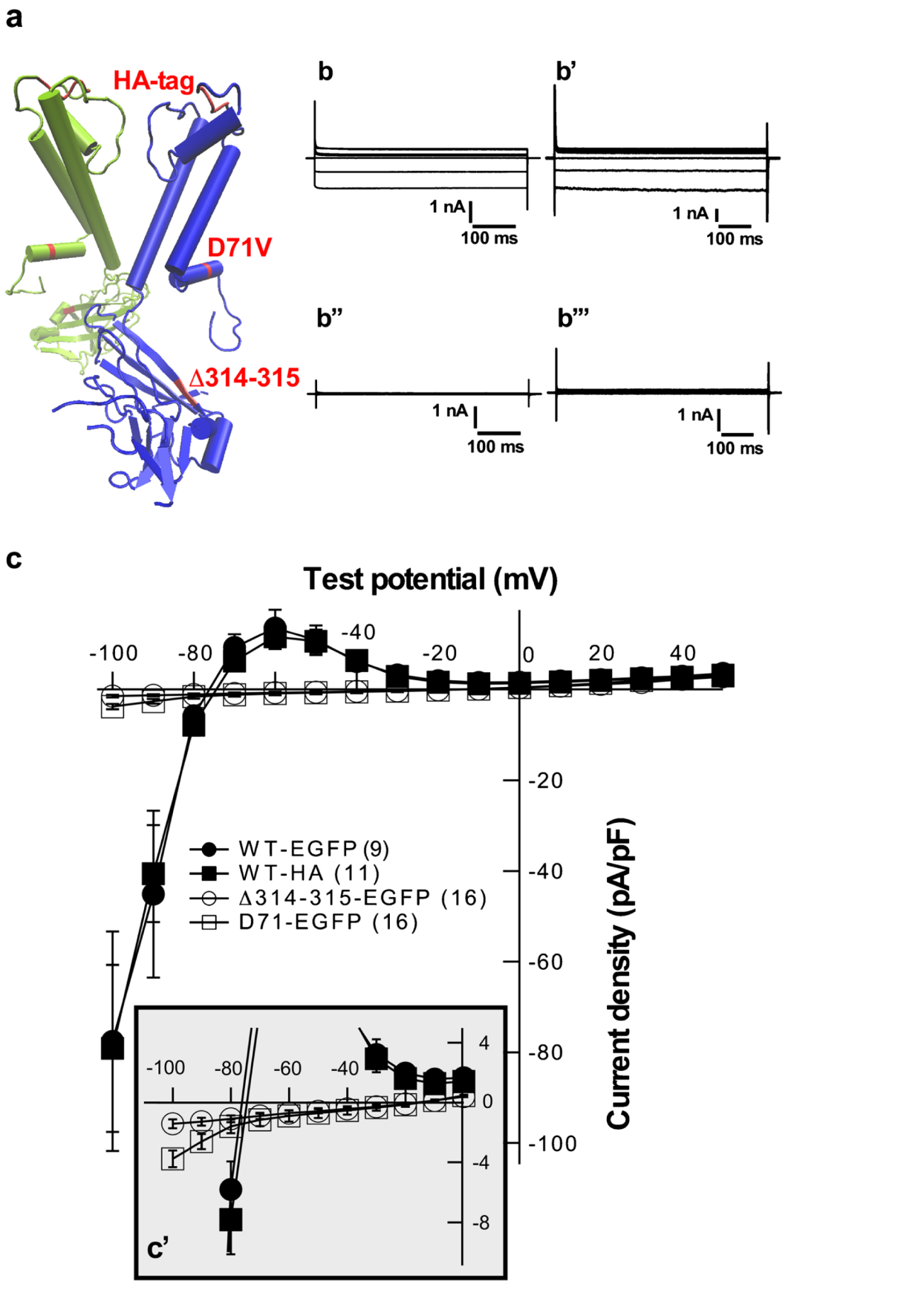

Fig. 1 Electrophysiological properties of COS-7 cells transduced with adenoviral- $K_{IR}2.1$ channels. **a** The relative locations of the two Andersen's syndrome mutations (D71V and Δ314-315) and the HA tag are shown on two subunits of the Kirbac1.1 crystal structure. The EGFP was fused to the C terminal part of the channel. **b** Representative current traces of COS-7 cells that were transduced Ad-WT-EGFP (**b'**), Ad-WT-HA (**b"**), Ad-Δ314-315-EGFP (**b"'**) and Ad-D71V-EGFP (**b"'**) constructs. Cells were held at −80 mV and depolarized to a series of voltage steps from −100 mV to +50 mV. **c** Current density–voltage relationship of COS-7 cells transduced and recorded as described in (**b**). *n* the number of cells recorded. Data are mean ± SEM. *Inset* an expansion of the same figure between −120 mV and 0 mV test potentials

Electrophysiology

Current recordings were conducted in the whole-cell voltage-clamp configuration at room temperature (~24 °C), (Hamill et al. 1981) using an EPC 10 amplifier (HEKA Electronic). The pipette solution contained (mM): 150 KCl, 0.5 $MgCl_2$, 5 EGTA and 10 HEPES, pH 7.3, 290 mOsm. The bathing medium was (mM): 150 NaCl, 5 KCl, 2 $CaCl_2$, 1 $MgCl_2$ and 10 HEPES, pH 7.3, 305 mOsm. Pipette resistance was 1.5-3 MΩ. Membrane currents were elicited by 500-ms depolarizations ranging from −100 mV to +50 mV, from a holding potential of −80 mV. Only cells with series resistance less than 5 MΩ were used for analysis. Data acquisition and analysis were performed using Patchmaster and Fitmaster (HEKA Electronic) and IgorPro (WaveMetrics) (Sacco et al. 2014; Sacconi et al. 2009).

Skeletal muscle transduction and extraction

All experiments were performed in accordance with the guidelines of the French Ministry of Agriculture (87/848) and of the European Community (86/609/EEC). Two-day-old OF1 mice were injected using a microelectrode in the *tibalis anterior* and *flexor digitorum brevis* muscles, with one of the adenovirus constructs carrying the WT $K_{IR}2.1$ or AS associated $K_{IR}2.1$ channel mutants fused to EGFP or HA tag. After 10 days of adenovirus expression, the *tibialis* muscles were extracted for immunohistochemistry (IHC) and confocal visualization.

Immunohistochemistry

For IHC, mice were first anesthetized with pentobarbital (80 mg/kg) and perfused with PBS followed by 4% paraformaldehyde (PFA) to fix the muscles. The *tibialis* muscles were then extracted and incubated in 4% PFA for several hours and then transferred to a 30% sucrose in PBS solution overnight at 4 °C. The next day, these muscles were frozen in OTC freezing media at −40 °C (using isopentane cooled with dry ice). The frozen tissue was then sliced (longitudinally) in 10-μm sections using a Microm HM505E cryostat.

The slices were transferred to glass slides and fixed with 4% paraformaldehyde, then permeabilized with 1% Triton, 0.1% SDS in PBS and blocked with 10% horse serum in PBS. Primary antibodies were used for different muscle markers such as rabbit polyclonal ryanodine receptor (from Dr. Lacampagne; 1:100 dilution), mouse monoclonal DHPR (Affinity Reagent; #MA3-920, 1:100 dilution), mouse monoclonal dystrophin (DYS) (Novocastra Laboratories; #NCL-DYS2; 1:10 dilution), nuclear marker DAPI, rabbit polyclonal anti-HA tag (Abgent Interchim; #ap1012a, 1:100 dilution). After incubation with primary antibodies, the slides were washed and incubated with secondary antibody Alexa fluor 594 (Invitrogen; 1:250 dilution). Confocal microscopy (Leica TCS SP5) was used to visualize fluorescence. Each immunohistochemical staining was performed at least three times with each antibody. The selected images presented in Figs. 2, 3, 4, 5 and 6 are representative from a series of 8 transduction trials in which each viral construct or pair of constructs (e.g., GFP-tagged/HA-tagged) was injected in 3 mice.

In vivo muscle fiber voltage clamp electrophysiology

Flexor *digitorum brevis* muscles were removed from 20-day-old male OF1 mice. Single fibers were isolated by a 50-min enzymatic treatment at 37 °C using a Tyrode solution containing 2 mg/mL collagenase type I (Sigma Aldrich). The Tyrode solution contained (mM) 140 NaCl, 5 KCl, 2.5 $CaCl_2$, 1 $MgCl_2$ and 10 HEPES adjusted to pH 7.2.

The major part of a single fiber was electrically insulated with silicone grease and a micropipette was inserted into the fiber through the silicone layer to voltage-clamp the portion of the fiber free of grease (50–100 μm length) using a patch-clamp amplifier (Bio-Logic RK-400) in whole-cell configuration (Collet et al. 2004). The pipette solution contained (mM): 120 K-glutamate, 5 Na_2-ATP, 5 Na_2-phosphocreatine, 5.5 $MgCl_2$, 5 glucose, 5 HEPES adjusted to pH 7.2. $BaCl_2$ was added to the external solution at a final concentration of 0.5 mM. Cells were exposed to different solutions by placing them by the mouth of a gravity-fed, rapid solution exchange perfusion tube. Experiments were carried out at room temperature (24 °C).

For Ad-D71V-EGFP- and Ad-Δ314-315-EGFP-positive fibers, the most fluorescent portion was left free of grease to focus measurements on the highest expressing region of the fiber. Command voltage and current acquisition were done using the pClamp10 software (Axon Instruments) driving an A/D converter (Digidata 1400A; Axon Instruments). Analog compensation was systematically used to decrease the effective series resistance. Cell capacitance was determined by integration of a current trace obtained with a 10-mV hyperpolarizing pulse from the holding potential preceding the voltage ramp protocol and was used to calculate the density of currents (A/F). Muscle fibers were held at −80 mV and stimulated every minute by a voltage ramp protocol consisting of a hyperpolarizing pulse to −120 mV during 200 ms followed by a depolarization ramp from −120 to −20 mV given at a rate of 20 mV/s.

Muscle isometric force measurements

For isometric muscle contraction studies, intact *extensor digitorum longus* (EDL) muscles were manually isolated, dissected and immediately placed in a custom-built Plexiglas chamber filled with Tyrode solution (121 mM NaCl, 5.0 mM KCl, 1.8 mM $CaCl_2$, 0.5 mM $MgCl_2$, 0.4 mM

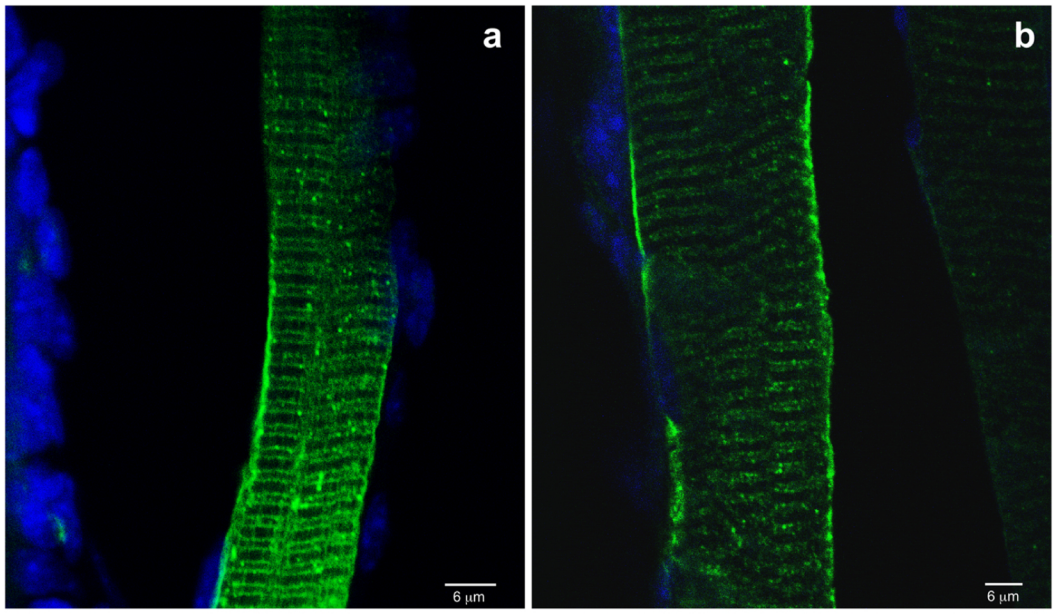

Fig. 2 EGFP and HA tags do not interfere with adenovirus-mediated wild-type (WT) $K_{IR}2.1$ channel expression in mouse *tibialis* muscle. Following transduction in mouse *tibialis* muscle, WT-EGFP (**a**) and WT-HA (**b**) are subcellularly distributed in the sarcolemma membrane and the T-tubules as determined by confocal microscopy. For HA detection, immunostaining with anti-HA antibody was applied

NaH_2PO_4, 24 mM $NaHCO_3$, 0.1 mM EDTA, 5.5 mM glucose) equilibrated with 95% O_2–5% CO_2 gas and maintained at 25 °C. The pH was set to 7.4. The muscle was attached at both tendons, one being a fixed point and the other connected to a force transducer/length servomotor system (model 305B; Cambridge Instruments, Aurora Scientific, Ontario, Canada). After 15-min equilibration in the bath, the muscle was stimulated along their entire length with platinum wire electrodes and the optimum muscle length (L0), i.e., the muscle length producing maximal twitch tension, was determined. All subsequent measurements were made at L0. The tension-frequency response was then determined (701B Stimulator; Aurora Scientific) using stimulation trains of 500 ms, with a pulse duration of 0.5 ms at frequencies of 1–

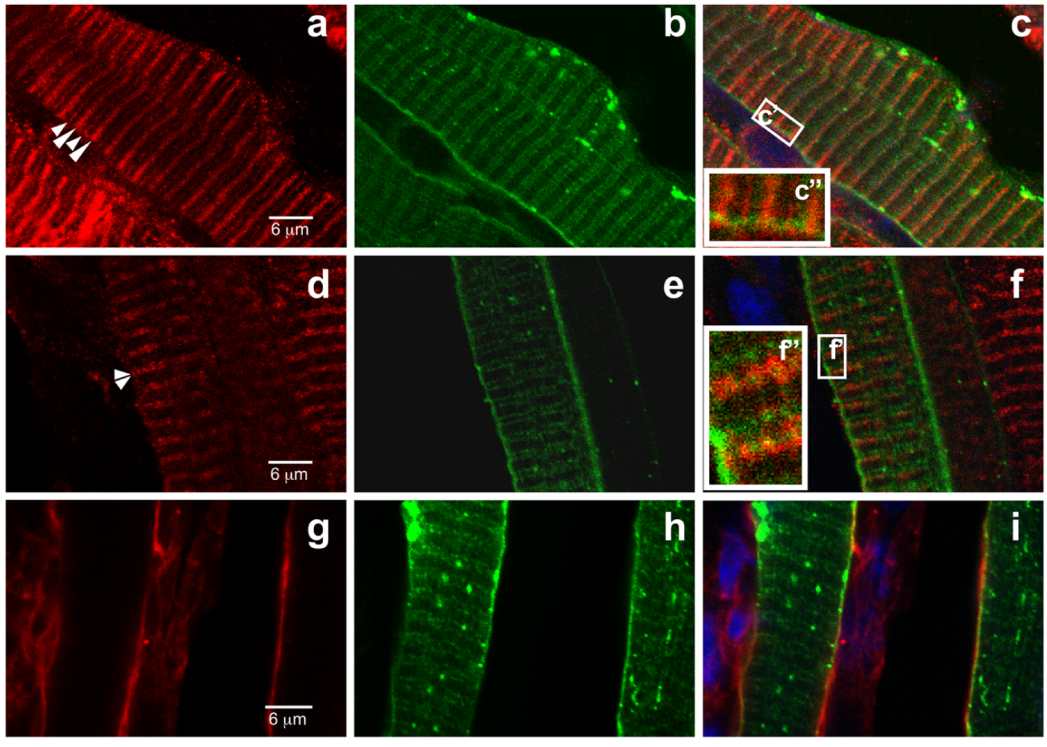

Fig. 3 The subcellular distribution of Ad-WT-EGFP is resolved with muscle tissue markers in mouse *tibialis* muscle. Confocal microscopy of mouse *tibialis* muscles that were transduced with Ad-WT-EGFP (*green*). Tissue slices were stained with antibodies directed against muscle markers (*red*) to localize $K_{IR}2.1$ in the subcellular compartments: ryanodine receptor (RyR) localized primarily in the sarcoplasmic reticulum membrane (**a**–**c**); dihydropyridine receptor (DHPR) localized in the T-tubule membranes (**d**–**f**); dystrophin found at the interface of the cytoskeleton and plasma membrane (**g**–**i**). The nuclei are stained with DAPI (*blue*). *Arrows* indicate the bands of staining that represent the sarcoplasmic reticulum membrane with RYR (**a**) and T-tubule membrane with DHPR (**d**) staining. *Insets* (**c'**, **f'**) show increased magnification of Kir2.1-EGFP localization with RYR (**c"**) or DHPR (**f"**)

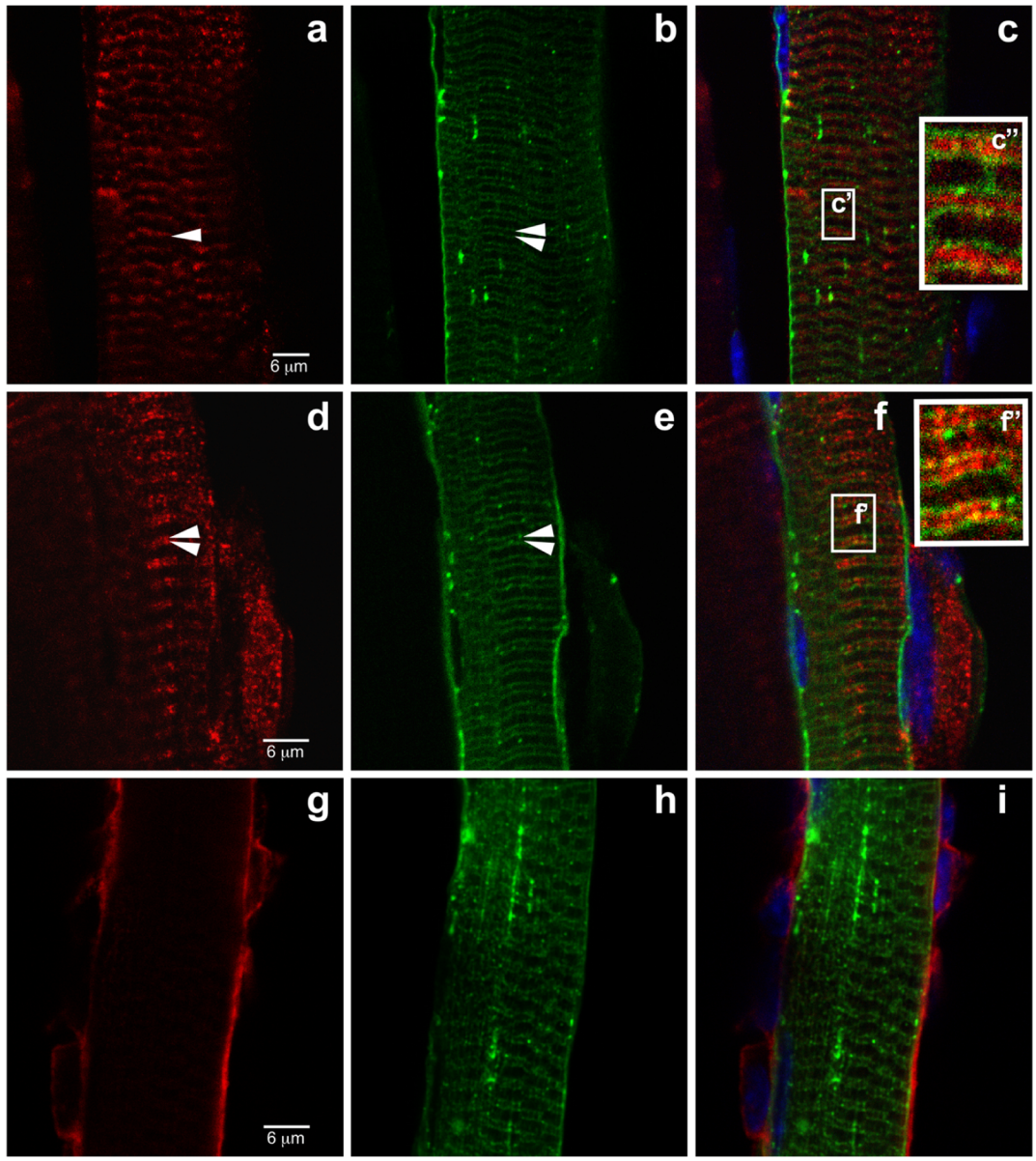

Fig. 4 Ad-D71V-EGFP AS mutant channel localization is similar to wild-type (WT) in mouse *tibialis* muscle. RyR (**a**–**c**), DHPR (**d**–**f**) and DYS (**g**–**i**) antibodies (*red*) were used to localize the Andersen's syndrome associated mutant D71V-EGFP (*green*) in the sarcolemma membrane and T-tubules similar to the WT $K_{IR}2.1$ channels. The nuclei are stained with DAPI (*blue*). *Arrows* indicate the bands of staining that represent the sarcoplasmic reticulum membrane with RYR and T-tubule membrane with DHPR staining. *Insets* (**c'**, **f'**) show increased magnification of Kir2.1-D71V-EGFP localization with RYR (**c"**) or DHPR (**f"**). *Right panels* are merged images of the *green*, *red* and *blue*

100 Hz. Stimulus trains were separated by 1-min intervals. The maximum isometric tetanic tension (P0) was then determined. After all measurements, muscles were removed from the bath, trimmed of the connective tissue, blotted dry and weighed on an analytical scale. The specific force (sP0, expressed in mN/mm^2) in each contraction was calculated by dividing the tension (P0) by the whole-muscle cross-sectional area, where the cross-sectional area was computed as muscle wet weight divided by the product of muscle length and density (1.06 g/ml) (Yamada et al. 2006).

The specific force–frequency relationship was analyzed by stimulating the muscle at frequencies ranging from 1 to 100 Hz. Force during a fatigue protocol was assessed by applying 30-Hz, 300-ms trains every second for 300 s. Force values were normalized to the force developed during the first train of the protocol. A repeated measures two-way ANOVA was performed to compare the results of the AS mutant (Δ314-315 and D71V) to control (WT-EGFP and EGFP) groups. Functional force/fatigue data were collected from 3 separate cohorts of mice transduced with the 4 adenoviruses (Ad-EGFP, Ad-WT-EGFP, Ad-D71V-EGFP and Ad-Δ314-315-EGFP).

Results

Efficiency of adenovirus strategy

Transduction efficiency and biophysical functionality of adenovirus mediated gene transfer of $K_{IR}2.1$ constructs with EGFP or HA tags were first evaluated in COS-7 cells. The electrophysiological properties were assessed after transduction with Ad-WT-EGFP and Ad-WT-HA by using whole-cell voltage-clamp technique. The electrophysiological properties of COS-7 cells were similar after transduction with Ad-WT-EGFP and

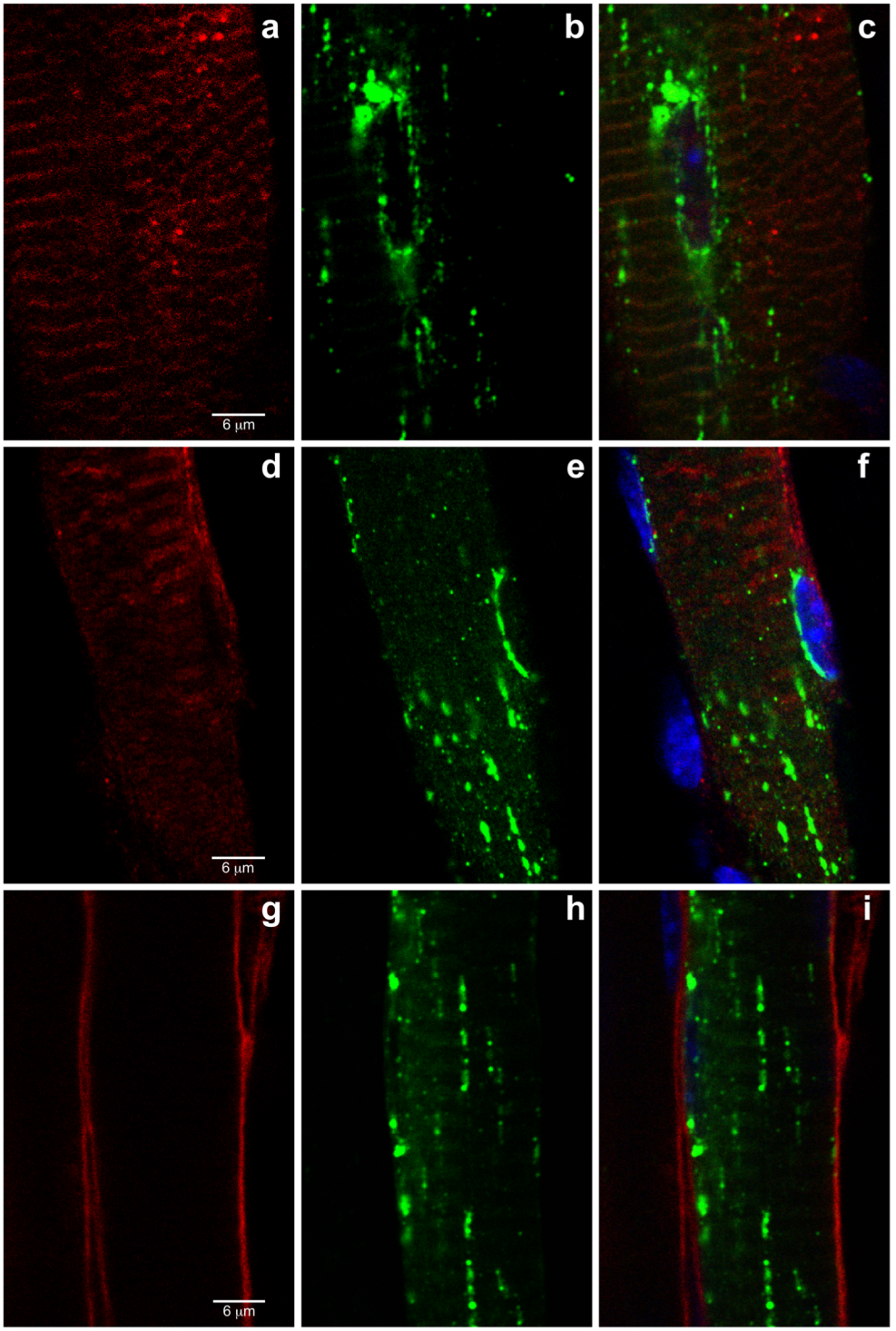

Fig. 5 Abnormal localization $K_{IR}2.1$ Δ314-315-EGFP AS mutation in mouse *tibialis* muscle. $K_{IR}2.1$ Δ314-315-EGFP AS mutant (*green*) does not localize in the sarcolemma membrane or the T-tubules like the wild-type. Instead it is seen in small vesicles throughout the muscle fiber. These channels do not co-localize with RyR (**a**–**c**), DHPR (**d**–**f**), or DYS (**g**–**i**; *red*). The nuclei are stained with DAPI (*blue*). *Right panels* are merged images of the *green*, *red* and *blue*

Ad-WT-HA (Fig. 1b, c) or transfection with WT-EGFP or WT-HA in a (non-viral) vector construct (Bendahhou et al. 2003). The inwardly rectifying K^+ current was present and was sensitive to 100 μM $BaCl_2$ (data not shown), in Ad-WT-EGFP- and Ad-WT-HA-transduced cells but was almost absent after Ad transduction with AS mutant $K_{IR}2.1$ channels (D71V-EGFP and Δ314-315-EGFP; Fig. 1b, c, inset).

Moreover, Ad-WT-EGFP and Ad-WT-HA expression in mouse *tibialis* muscle was consistently abundant on the cell surface and T-tubules as seen by visualizing both EGFP and HA tags (Fig. 2). The similarity in the expression of the WT $K_{IR}2.1$ channel with both tag types confirms that the tags (EGFP and HA) do not constrict channel function and WT channels are properly and

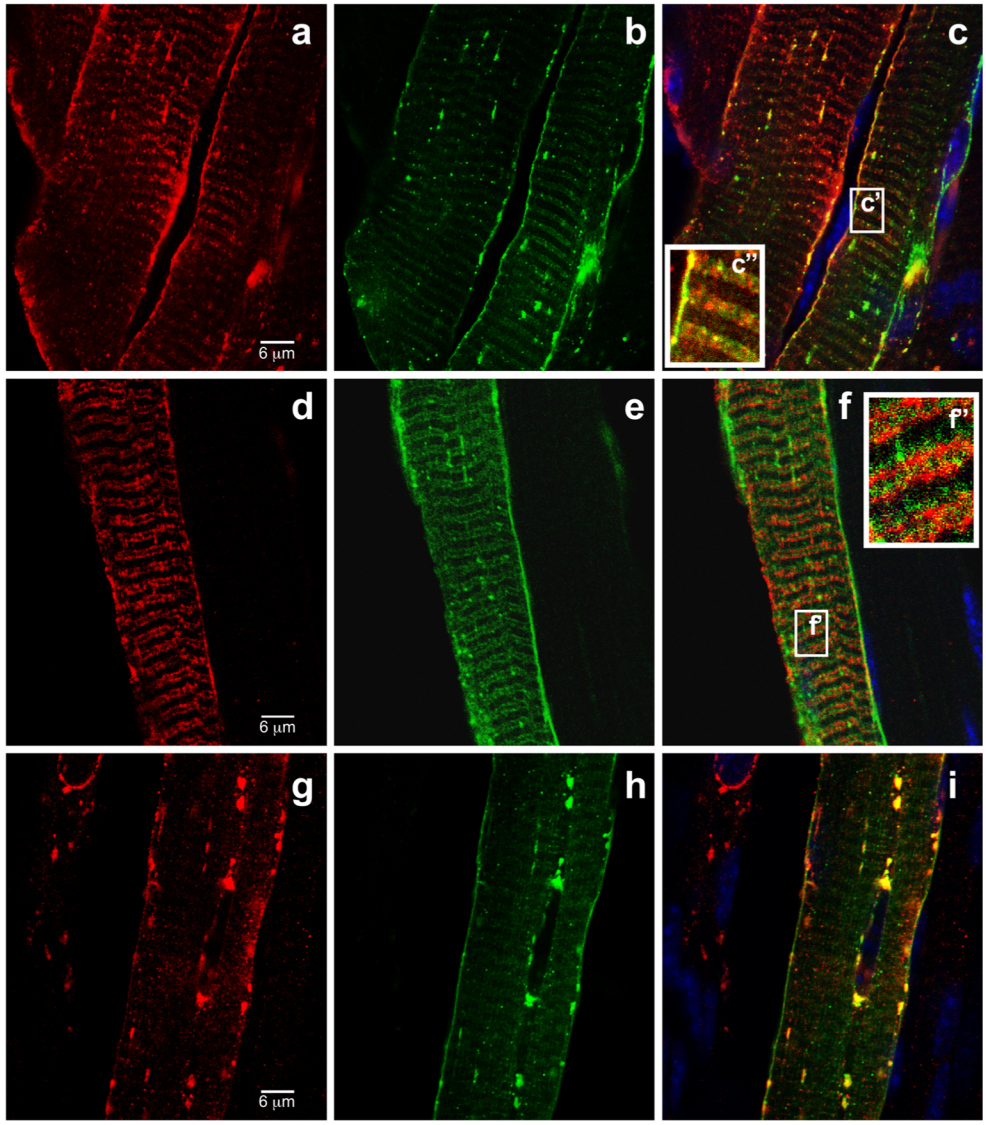

Fig. 6 Dominant-negative behavior of AS mutants in mouse skeletal muscle. Immunohistostaining and confocal microscopy were used to co-localize wild-type (WT) and mutant $K_{IR}2.1$ channels in mouse *tibialis* muscle. Both WT-HA (**a**–**c**) and D71V-HA (**d**–**f**) have clear co-localization with WT-EGFP and are localized at sarcolemma and T-tubule membranes. However, co-transduction with the Ad-Δ314-315-HA mutant and Ad-WT-EGFP lead to WT channels co-localizing with Δ314-315 that prevented them from reaching the membrane (**g**–**i**). The nuclei were stained with DAPI (*blue*). *Insets* (**c'**, **f'**) show increased magnification of Kir2.1-D71V-EGFP localization with RYR (**c"**) or DHPR (**f"**). *Right panels* are merged images of the *green*, *red* and *blue*

functionally expressed in the membrane, whereas selected AS $K_{IR}2.1$ mutations (D71V and Δ314-315) produce almost silent $K_{IR}2.1$ channels (Fig. 1b, c, inset).

Distribution of wild-type $K_{IR}2.1$ channels in skeletal muscle

Optical confocal microscopy was used to evaluate the subcellular distribution of EGFP-tagged WT $K_{IR}2.1$ channels after adenovirus transduction in mouse *tibialis anterior* skeletal muscle by co-localization with muscle compartment markers (Fig. 3). $K_{IR}2.1$ was abundant at the sarcolemma membrane and as regularly spaced transverse striations in skeletal muscle fibers. Co-localization of $K_{IR}2.1$ with DYS, a sarcolemma membrane matrix protein, further confirms proper trafficking of the $K_{IR}2.1$ channel to the sarcolemma membrane. $K_{IR}2.1$ WT channels were also resolved as double bands that appear co-localized with dihydropyridine receptor (DHPR; a marker of T-tubules) staining. Ryanodine receptor (a sarcoplasmic reticulum membrane marker) immunostaining was resolved as a double band in red, where one band is much brighter than the other (Fig. 3). Localization of $K_{IR}2.1$-EGFP with RYR is less pronounced than with DHPR as the two green EGFP fluorescing bands surround the brighter red Alexa 594 (secondary antibody) band. For this reason, we believe that $K_{IR}2.1$ is localized at the T-tubule membrane and not sarcoplasmic reticulum (SR) membranes. However, as RYR and DHPR in skeletal muscle are in very close proximity of each other, resolving precisely the Kir2.1 localization between T-tubule membranes and SR membranes requires much higher resolution imaging.

Distribution of Andersen's syndrome associated $K_{IR}2.1$ channel mutants in murine skeletal muscle

$K_{IR}2.1$ mutations, D71V and Δ314-315, have been previously identified to occur in subsets of Andersen's syndrome patients (Bendahhou et al. 2003). Hence, to determine the subcellular distribution pattern of mutant $K_{IR}2.1$ channels in vivo, Ad-D71V-EGFP and Ad-Δ314-315-EGFP were used to transduce skeletal muscle. Expression of $K_{IR}2.1$ channels carrying the D71V Andersen's mutation followed a similar pattern to WT channels as determined by co-localization with muscle subcellular compartment markers (Fig. 4). Thus, the D71V mutation does not interfere with proper trafficking of channel complexes to the T-tubule and sarcolemma membranes.

Conversely, the Δ314-315 mutation impedes the proper trafficking of $K_{IR}2.1$ channels to the membrane, capturing them in the internal compartments of the skeletal muscle fibers as shown in Fig. 5. These compartments cluster densely around the nuclei and also span the muscle fiber.

To show that $K_{IR}2.1$ trafficking and localization were not affected by its fusion to the EGFP, we tagged this channel in a different area using a smaller tag (HA tag; Fig. 1a). *Tibialis* muscles transduction with HA tagged WT and AS mutant channels produced a similar localization pattern to that observed with EGFP tagged channels (Figs. 2, 6).

Dominant-negative effect of AS $K_{IR}2.1$ mutants in muscle

Moreover, as Andersen's syndrome is associated with dominant negative mutations of the $K_{IR}2.1$ channel, to determine the effect of AS mutant expression on WT channels, mouse *tibialis* muscles were co-transduced with Ad-WT-EGFP and mutant channels Ad-D71V-HA or Ad-Δ314-315-HA and stained with anti-HA antibody. Figure 6 shows the precise co-localization of the WT-EGFP and WT-HA constructs in the mouse *tibialis* muscle at the sarcolemma membrane as well as the T-tubules. Also, co-transduction with Ad-D71V-HA does not prevent correct WT-EGFP expression in the muscle. Ad-D71V-HA and Ad-WT-EGFP have a similar localization pattern to that observed with co-localized WT-EGFP and WT-HA, neither of which prevent proper trafficking of the channel complex. However, co-transduction of Ad-WT-EGFP with Ad-Δ314-315-HA impedes on proper localization of WT channels in the sarcolemma and T-tubule membranes as WT-EGFP is co-localized with Δ314-315-HA (Fig. 6).

Adenoviral transduction with AS $K_{IR}2.1$ channel mutants silences K_{IR}-mediated conductance in mouse skeletal muscle

To assess the efficiency of our adenoviral constructs and to test our hypothesis that the adenoviral-induced animal model recapitulates the electrophysiological characteristics of AS and control human myocytes, untransduced control or Ad-Δ314-315-EGFP-transduced muscle fibers were challenged under voltage-clamp conditions by voltage ramps applied from −120 to −20 mV. The background current was explored in this negative membrane voltage range because it was expected to be mainly carried by the inward rectifier K^+ (K_{IR}) channels. Figure 7a presents the voltage dependence of the background current in control fibers in the presence of an external Tyrode solution. The current–voltage relationship was found to be linear between −120 and −80 mV and it was assumed that a fraction of this inward current should flow through K_{IR} channels. Indeed, addition of 0.5 mM Ba^{2+}, a very potent blocker of K_{IR} channels (Standen and Stanfield 1978), induced a marked reduction of the slope of the current–voltage relationship between −120 and −80 mV, suggesting that a substantial fraction of this part of the current was carried by K_{IR} channels. The fraction of inward current that remained after the addition of Ba^{2+} was not further investigated. Figure 7b shows the current recorded in an Ad-Δ314-315-EGFP-transduced muscle fiber. The slope of the current–voltage relationship between −120 and −80 mV was dramatically reduced and the addition of Ba^{2+} had little effect, suggesting that K_{IR} channel activity was almost entirely suppressed in this transduced cell. This difference in the slope of the current–voltage relationship was also clearly apparent when the mean current was plotted as a function of voltage in control and in Ad-Δ314-315-EGFP-transduced muscle fibers (Fig. 7c). Fitting a linear relationship between current and voltage in the −120 to −80 mV voltage range in each cell indicated a mean conductance of 154 ± 28 S/F in Ad-Δ314-315-EGFP-transduced muscle fibers (n = 14), which was found to be significantly reduced ($P < 0.05$) as compared to the mean conductance in control fibers (339 ± 35 S/F, n = 17). In order to better estimate the magnitude of the current carried by K_{IR} channels in control and in Ad-Δ314-315-EGFP-transduced muscle fibers, we subtracted the current that remained in the presence of Tyrode with 500 μM Ba^{2+} added from the current recorded in the presence of Tyrode in the same fiber and plotted as a function of voltage the current difference corresponding to the Ba^{2+}-sensitive component (Fig. 7a, b). Using this same procedure in each control and Ad-Δ314-315-EGFP-transduced muscle fibers indicated that the mean Ba^{2+}-sensitive current displayed a voltage-dependence reminiscent of the voltage-dependence expected for K_{IR} channels in control cells and that this mean current was considerably reduced in Ad-Δ314-315-EGFP-transduced muscle fibers (Fig. 7d). Fitting a linear relationship between current and voltage in each cell indicated a significantly reduced ($P < 0.05$) mean conductance for Ad-Δ314-315-EGFP-transduced muscle fibers (18 ± 4 S/F), as compared to control fibers (140 ± 20 S/

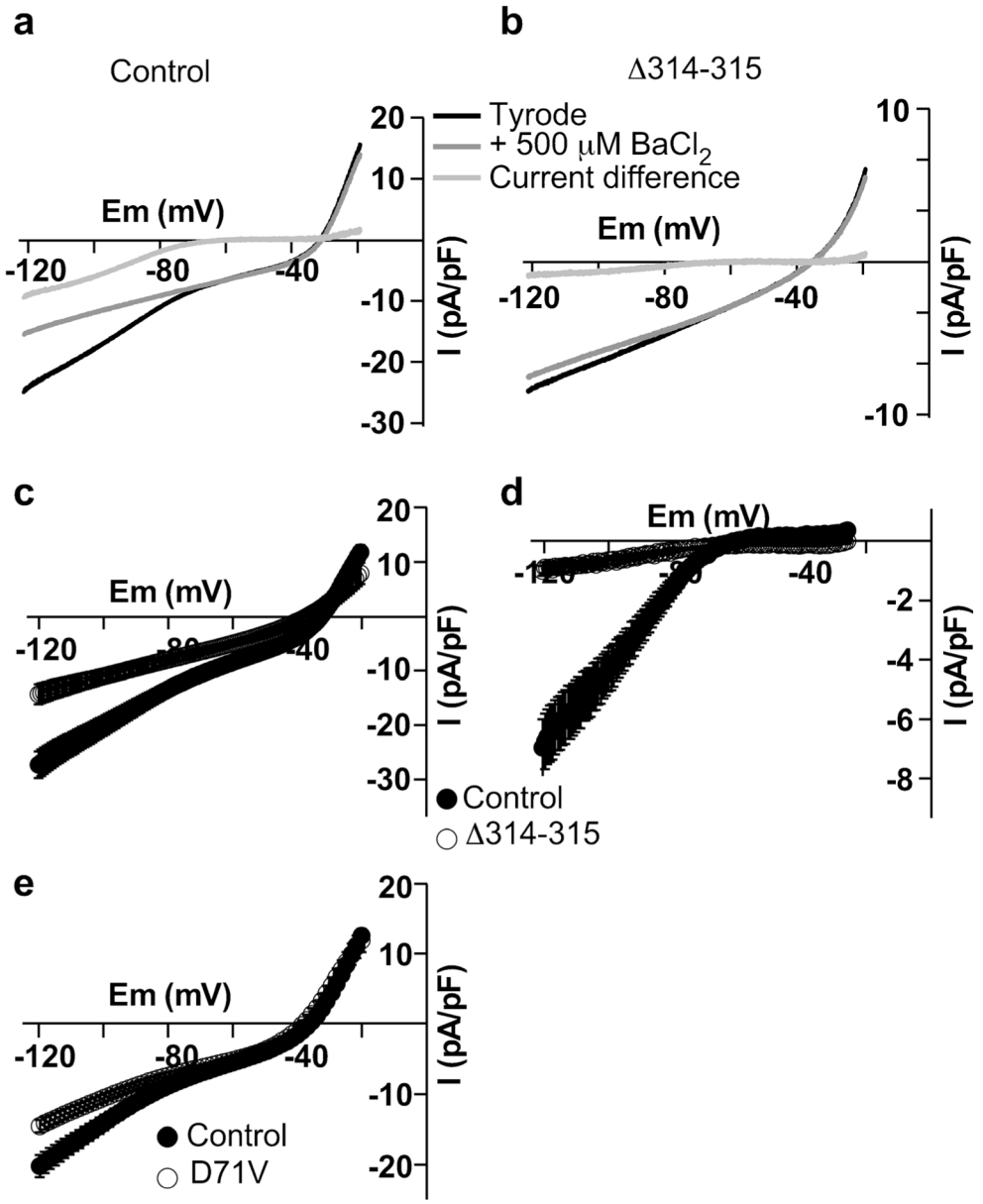

Fig. 7 KIR currents in control and Ad-Δ314-315-transduced mouse skeletal muscle fibers. **a** The currents were recorded in response to voltage ramps applied from −120 to −20 mV in the same control fiber in the presence of a Tyrode solution (*black*) and in the presence of a Tyrode solution +500 μM Ba^{2+} (*gray*). The current difference in *light gray* was obtained after subtraction of the current remaining in the presence of Tyrode with 500 μM Ba^{2+} to the current obtained in the presence of Tyrode without Ba^{2+}. **b** The same protocol was applied on an Ad-Δ314-315-EGFP-transduced muscle fiber. **c** The mean current and SEM obtained in 17 control (●) and 14 Ad-Δ314-315-EGFP-transduced muscle fibers (○) in response to voltage ramps in the presence of Tyrode were plotted as a function of voltage. **d** The mean and SEM of the current difference obtained using the same procedure as in (**a**) and (**b**) in 5 control and 4 Ad-Δ314-315-EGFP-transduced muscle fibers were plotted as a function of voltage. **e** The mean current and SEM obtained in 12 control (●) and 8 D71V-EGFP-transduced muscle fibers (○) in response to voltage ramps in the presence of Tyrode were plotted as a function of voltage. The number of data points has been reduced for clarity in (**c**) and (**d**)

F). The effect of the D71V mutation on Kir currents has also been investigated in a series of experiments by measuring, in control and in D71V-transduced fibers, the changes in background current induced by voltage ramps using the same protocol as for the Δ314-315 mutation. The mean current–voltage relationships obtained in control and D71V-transduced fibers are shown in Fig. 7e. As observed for the Δ314-315 mutation, the D71V mutation induced a very significant reduction of the Kir conductance measured between −120 and −80 mV from 293 ± 26 S/F (n = 12) in control to 182 ± 17 S/F (n = 8) in D71V-transduced fibers (P = 0.006). These data confirm that the Δ314-315 and the D71V mutations induce an almost complete inhibition of K_{IR} activity in muscle cells.

AS K_{IR}2.1 channel mutants impair muscle isometric contraction and resistance to fatigue

Finding K_{IR}2.1 channel expression at the T-tubule membranes may signify a role of this channel in the excitation-contraction coupling. Also, it has been classically observed, that during chronic as well as inherited muscle diseases, muscle dysfunction occurs characterized by muscle remodeling (slow to fast twitch transition) associated with altered contractility and increased muscle fatigue. This has been previously found to be associated with altered calcium signaling in the excitation–contraction coupling cascade (Reiken et al. 2003; Ward et al. 2003). To determine the correlation between the K_{IR}2.1 function and the excitation–contraction coupling mechanism in skeletal muscle and the effect of AS-associated K_{IR}2.1

mutations on skeletal muscle mechanics, functional studies were performed on $K_{IR}2.1$ adenovirus-transduced mouse skeletal muscle.

The force–frequency relationship was analyzed in isometric conditions, which is typically carried out to evaluate muscle resistance or fragility in response to rapid stretch in various myopathies. Isometric force production was measured as a function of stimulation frequency (Fig. 8) in WT EDL muscle infected with EGFP and Ad-WT-EGFP and AS mutants Ad-D71V-EGFP and Ad-Δ314-315-EGFP. Expression of AS mutant channels resulted in a ~40% decrease in specific force production at frequencies between 60 and 100 Hz (Fig. 8a). A decreased force generation in response to certain frequencies has been suggested to be a result of either decreased sensitivity of the contractile apparatus to Ca^{2+} or decreased magnitude of Ca^{2+} transients for each activating pulse. The resistance to fatigue was also found significantly reduced for Δ314-315 and showed a trend for the D71V compared to WT (Fig. 8b). A reduced resistance to fatigue can also be due to a reduction in Ca^{2+} release or metabolic impairments.

Discussion

In this study, we investigated the cellular localization, trafficking and the protein interactions of the inwardly rectifying $K_{IR}2.1$ channel in the skeletal muscle. Mutations of this channel are associated with AS, a disorder presenting with periodic paralysis, cardiac arrhythmias and dysmorphic features. In this disorder, mutations of the $K_{IR}2.1$ produce a silent channel and abolish the inwardly rectifying current in muscle fibers. Several mechanisms by which $K_{IR}2.1$ channel mutations abolish channel function have previously been identified including channel misfolding, problematic trafficking, improper interaction with other cellular proteins or lipids and potential structural instability of the channels in the membranes producing silent channels (Ballester et al. 2006, 2007; Bendahhou et al. 2003; Donaldson et al. 2003; Lim et al. 2010; Tan et al. 2012). Our goal was to shed the light on the role of this channel in vivo and on the mechanisms through which AS-associated $K_{IR}2.1$ channel mutations lead to periodic paralysis and cardiac arrhythmias.

The two AS mutations studied here have been reported earlier (Plaster et al. 2001) and the patients were all classified as being AS because they exhibited the AS triad: periodic paralysis, cardiac arrhythmia and developmental features. We have shown that both D71V and Δ314-5 mutations led to a loss of function in vitro (Bendahhou et al. 2003). Furthermore, we found no relationship between genotype and phenotype among AS patients carrying different mutations (Tristani-Firouzi et al. 2002). These two mutations were chosen because they represent the two major mechanisms by which the loss of Kir2.1 function occurs: silent channels at the cell surface (D71V) and mistrafficking (Δ314-315).

Using the adenovirus strategy to express $K_{IR}2.1$ channels in mouse skeletal muscle, we were able to directly localize these channels in the sarcolemma membrane and transverse tubules. Although $K_{IR}2.1$ is expressed endogenously in mouse, the use of the adenovirus-expressing $K_{IR}2.1$ channels with fluorescent tags allowed us to properly visualize these channels without the use of $K_{IR}2.1$-directed antibodies. Granted, other viral strategies are available, as the adenovirus has been shown to provide the moderate expression efficiency necessary to properly localize these channels in specific cellular compartments. If overexpression was more pronounced, we may have seen $K_{IR}2.1$ channels everywhere in the fiber; however, this was not the case with WT, D71V or Δ314-315 AS-associated mutants. WT $K_{IR}2.1$ and D71V mutant channels were localized in specific areas such as the T-tubules and sarcolemma membrane while the Δ314-315 AS mutation prevented the channel from being properly trafficked to the membrane. This AS mutant channel was retained in small vesicular subcellular compartments throughout the fiber and not along the membranes of either sarcolemma or T-tubules. Previous in vitro studies demonstrated that $K_{IR}2.1$ channels co-localize with markers of the medial- and trans-Golgi and that the Δ314-315 mutation blocks trafficking of these channels into the Golgi apparatus (Ma et al. 2011). As $K_{IR}2.1$ channel subunits must be formed into tetramers before reaching the membrane, a mutation in a trafficking site of even one subunit can trap the whole channel complex in the intracellular compartments of the muscle fiber intended for degradation. Hence, these data clearly illustrate the dominant negative nature of these AS mutations on WT channels in a cell culture system and supports our findings in vivo.

The use of antibodies against specific skeletal muscle markers allowed us to co-localize the $K_{IR}2.1$ channel within specific compartments in the muscle. Since DYS is a sarcolemma membrane matrix protein, an anti-DYS antibody was used to co-localize $K_{IR}2.1$ WT and the D71V mutant in the sarcolemma membrane. While the distance between a ryanodine receptor, a sarcoplasmic reticulum membrane channel and DHPR, a T-tubule membrane channel, is extremely small owing to their direct interaction, a difference in localization is still observed when comparing these two markers with $K_{IR}2.1$ localization. Indeed, DHPR seems to be more closely localized to $K_{IR}2.1$ than to the ryanodine receptor (Fig. 3). The use of confocal imaging to visualize expression of a channel is a highly effective technique with strong resolution; however, it is not possible to exactly pin-point $K_{IR}2.1$ localization in the T-tubule membrane and associate it with DHPR without the higher resolution possible with an electron microscope.

The role of the $K_{IR}2.1$ channel in skeletal muscle has not been sufficiently explained. Inwardly rectifying K^+ channels have been thought to primarily set the resting membrane

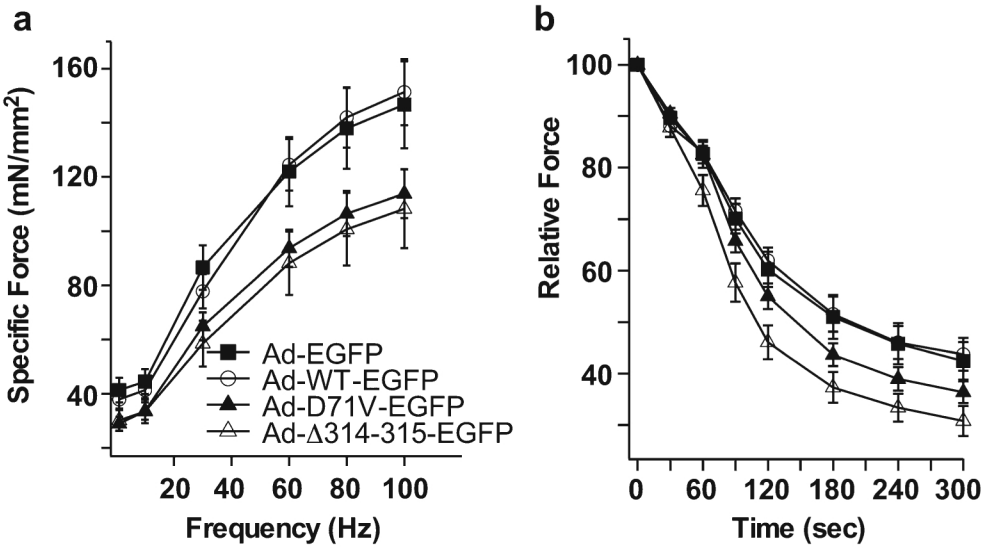

Fig. 8 AS $K_{IR}2.1$ channel mutants impair isometric contraction and resistance to fatigue in muscle. **a** Specific force–frequency relationship of mouse *EDL* muscles transduced with Ad-Δ314-315-EGFP $K_{IR}2.1$ mutant channels shows a significantly decreased force produced in response to different frequency stimulations from 1 Hz to 100 Hz when compared to WT (repeated measures ANOVA: $P < 0.005$). **b** Ad-Δ314-315-EGFP-transduced mouse *EDL* muscles show a significantly reduced force during a fatigue protocol (30 Hz, 300-ms trains applied every second for 5 min). Force values are normalized to the force developed during the first train of the protocol (repeated measures ANOVA: $P < 0.005$). One EDL muscle was used from each animal and numbers for each protocol are in parentheses next to corresponding adenovirus treatment group

potential in skeletal muscle. However, our discovery of $K_{IR}2.1$ channels in the T-tubular system may imply that these channels have yet another function in the excitation–contraction coupling mechanism. The T-tubular system and the sarcoplasmic reticulum are specialized compartments that contain the excitation–contraction coupling machinery necessary for proper skeletal muscle function. When an action potential is generated in the neuromuscular junction at the sarcolemma membrane, the depolarization of the membrane potential propagates to the T-tubules by the activation of voltage-gated Na^+ channels resulting in an inward Na^+ current. The voltage-gated Ca^{2+} channel DHPR senses this voltage change and begins the calcium signaling cascade by opening ryanodine receptors, thus triggering the release of Ca^{2+} from the SR into the cytosol to initiate a muscle contraction (Dulhunty et al. 2002). To repolarize the muscle fiber and bring membrane potential back to the resting value, K^+ ions exit the cell by voltage-gated K^+ channels at more depolarized potentials and accumulate in the extracellular T-tubular space (Sejersted and Sjogaard 2000). It is suggested that inwardly-rectifying K^+ channels may also have a role in this outward K^+ movement. As the concentration of extracellular K^+ increases, the tubular resting membrane potential would be positively shifted; however, as inward chloride conductance is very high in skeletal muscle during this repolarization phase, the resting membrane potential is balanced and prevented from becoming too depolarized. At the same time, inward transport of K^+ is initiated by the Na^+/K^+ pump as well as K_{IR} channels to bring the resting membrane potential back to more negative potentials, in order to maintain proper action potentials (Adrian and Bryan, 1974; Adrian et al. 1970; Adrian and Marshall 1976; Almers 1972; DiFranco et al. 2015). During this repolarization phase and after a contraction has occurred, Ca^{2+} is actively pumped back into the sarcoplasmic reticulum by the Ca^{2+}-ATPase SERCA pump. Proper Ca^{2+} signaling cascade function is ensured by ion channels and proteins closely localized in the T-tubules and sarcoplasmic reticulum. Thus, more work is required to determine the role of $K_{IR}2.1$ in the excitation–contraction coupling cascade and the use of our adenoviral strategy allows more precise measurements of channel interactions and functions for future experimentation. However, our contractile measurement strongly suggests that an improper repolarization to normal resting potential may partially inactivate the EC coupling process resulting in lower force production, as observed here with the mutant channels on the isometric force–frequency relationship.

As $K_{IR}2.1$ channel knockout mice die within several hours of birth, use of them as a model to study AS is unlikely. Previous studies have relied on in vitro or ex vivo systems to investigate $K_{IR}2.1$ channel function and the effects of silencing channel through AS-associated mutations. The functional assays performed here on skeletal muscle fibers that were transduced with AS mutant channels show an almost complete knockdown of the K_{IR} component, thus our data demonstrate that we have generated a good in vivo model for AS. Our system offers a unique tool to investigate skeletal muscle pathophysiology in vivo with implications not only for AS but also for other dominantly-inherited disorders.

Kir2.1 channels are widely expressed in human tissues but specifically in skeletal and cardiac muscles. This was highlighted by AS complex clinical phenotypes. A single amino acid change on the Kir2.1 channel leads to a loss of K^+ current flow that would depolarize resting membrane potentials in these tissues. This would put voltage-gated sodium channels (Nav1.4 in skeletal muscle and Nav1.5 in the heart) in an inactivated state. During repetitive action potentials in skeletal muscle, there is a build-up of K^+ ions in the tubular interspace, due to the activity of the voltage-dependent K^+ channels that contribute to the repolarization phase. This may lead to a persistent depolarization in this region that further inactivates Nav1.4 channels. This would cause a failure in action potential propagation, leading to periodic paralysis. In cardiac muscle and specifically in the ventricular compartment, where the action potential has a long repolarization phase and Kir2.1 intervenes not only in establishing the resting membrane potential but also in the late repolarization of the ventricular action potential, leading to cardiac arrhythmia.

We measured the specific force developed during an isometric contraction of the skeletal muscle by different frequency stimulations. Figure 8a shows a significant reduction in force developed by the AS mutant channel-transduced muscles. Although there are several factors that can affect muscle force, one of the major ones is the amount of Ca^{2+} released from the sarcoplasmic reticulum during a contraction stimulation and the Ca^{2+} gradient between the cytosol and the sarcoplasmic reticulum at the time Ca^{2+} is released (Chew et al. 2002; Citi and Kendrick-Jones 1987; Endo 1972; Movsesian and Schwinger 1998). Other factors involve muscle length at the sarcomeres and the amount of motor units. Our results were normalized to muscle length when the muscle was stretched as well as the weight of the muscles used. As the EDL muscle is mostly a fast twitch muscle, ATP from glycolysis is required to fuel its activity. ATP metabolism and activity on the other hand was not accounted for in our experiments.

Furthermore, we measured the susceptibility of EDL muscles to fatigue in $K_{IR}2.1$ WT or AS mutants. A significant difference was found between the WT and the Δ314-315 mutant (Fig. 8b). This is also a good indicator of the fact that these channels have a role in the excitation–contraction coupling mechanism. Many studies suggest that fatigue is a result of changes in excitability, reactive oxygen species and metabolic changes as well as interruptions in cross-bridge cycling of myosin and actin (Allen et al. 1992, 2008a, b; Allen and Westerblad 2001; Fitts 1994). Thus, our conclusion is that $K_{IR}2.1$ is important in the excitation–contraction coupling mechanism and its role in skeletal muscle should be further studied.

Acknowledgments This work was supported by the Centre National de la Recherche Scientifique (CNRS) and Association Française contre les Myopathies (AFM) grant (S.B.) and Chateaubriand fellowships (D.S.) and City of Nice fellowship (S.G. and A.V.). We thank the Vector Core of the University Hospital of Nantes for providing the adenovirus vectors.

Conflict of interest The authors declare having no conflict of interest.

References

Adrian RH, Bryant SH (1974) On the repetitive discharge in myotonic muscle fibres. J Physiol 240:505–515

Adrian RH, Chandler WK, Hodgkin AL (1970) Voltage clamp experiments in striated muscle fibres. J Physiol 208:607–644

Adrian RH, Marshall MW (1976) Action potentials reconstructed in normal and myotonic muscle fibres. J Physiol 258:125–143

Allen DG, Lamb GD, Westerblad H (2008a) Impaired calcium release during fatigue. J Appl Physiol 104:296-305

Allen DG, Lamb GD, Westerblad H (2008b) Skeletal muscle fatigue: cellular mechanisms. Physiol Rev 88:287-332

Allen DG, Westerblad H (2001) Role of phosphate and calcium stores in muscle fatigue. J Physiol 536:657–665

Allen DG, Westerblad H, Lee JA, Lannergren J (1992) Role of excitation-contraction coupling in muscle fatigue. Sports Med 13:116-126

Almers W (1972) Potassium conductance changes in skeletal muscle and the potassium concentration in the transverse tubules. J Physiol 225: 33–56

Andersen ED, Krasilnikoff PA, Overvad H (1971) Intermittent muscular weakness, extrasystoles, and multiple developmental anomalies. A new syndrome? Acta Paediatr Scand 60:559–564

Ashcroft FM, Heiny JA, Vergara J (1985) Inward rectification in the transverse tubular system of frog skeletal muscle studied with potentiometric dyes. J Physiol 359:269–291

Ashen MD, O'Rourke B, Kluge KA, Johns DC, Tomaselli GF (1995) Inward rectifier K+ channel from human heart and brain: cloning and stable expression in a human cell line. Am J Phys 268:H506–H511

Ballester LY, Benson DW, Wong B, Law IH, Mathews KD, Vanoye CG, George AL Jr (2006) Trafficking-competent and trafficking-defective KCNJ2 mutations in Andersen syndrome. Hum Mutat 27:388

Ballester LY, Vanoye CG, George AL, Jr. (2007) Exaggerated Mg2+ inhibition of Kir2.1 As a consequence of reduced PIP2 sensitivity in Andersen syndrome. Channels (Austin) 1:209-217

Bendahhou S, Donaldson MR, Plaster NM, Tristani-Firouzi M, Fu YH, Ptacek LJ (2003) Defective potassium channel Kir2.1 Trafficking underlies Andersen-Tawil syndrome. J Biol Chem 278:51779–51785

Chew TL, Wolf WA, Gallagher PJ, Matsumura F, Chisholm RL (2002) A fluorescent resonant energy transfer-based biosensor reveals transient and regional myosin light chain kinase activation in lamella and cleavage furrows. J Cell Biol 156:543–553

Christe G (1999) Localization of K(+) channels in the tubules of cardiomyocytes as suggested by the parallel decay of membrane capacitance, IK(1) and IK(ATP) during culture and by delayed IK(1) response to barium. J Mol Cell Cardiol 31:2207–2213

Citi S, Kendrick-Jones J (1987) Regulation of non-muscle myosin structure and function. BioEssays 7:155–159

Clark RB, Tremblay A, Melnyk P, Allen BG, Giles WR, Fiset C (2001) T-tubule localization of the inward-rectifier K(+) channel in mouse ventricular myocytes: a role in K(+) accumulation. J Physiol 537: 979–992

Collet C, Pouvreau S, Csernoch L, Allard B, Jacquemond V (2004) Calcium signaling in isolated skeletal muscle fibers investigated under "silicone voltage-clamp" conditions. Cell Biochem Biophys 40:225–236

DiFranco M, Yu C, Quinonez M, Vergara JL (2015) Inward rectifier potassium currents in mammalian skeletal muscle fibres. J Physiol 593:1213–1238

Donaldson MR, Jensen JL, Tristani-Firouzi M, Tawil R, Bendahhou S, Suarez WA, Cobo AM, Poza JJ, Behr E, Wagstaff J, Szepetowski P, Pereira S, Mozaffar T, Escolar DM, Fu YH, Ptacek LJ (2003) PIP2 Binding residues of Kir2.1 Are common targets of mutations causing Andersen syndrome. Neurology 60:1811–1816

Doupnik CA, Davidson N, Lester HA (1995) The inward rectifier potassium channel family. Curr Opin Neurobiol 5:268–277

Dulhunty AF, Haarmann CS, Green D, Laver DR, Board PG, Casarotto MG (2002) Interactions between dihydropyridine receptors and ryanodine receptors in striated muscle. Prog Biophys Mol Biol 79: 45–75

Endo M (1972) Stretch-induced increase in activation of skinned muscle fibres by calcium. Nat New Biol 237:211–213

Fitts RH (1994) Cellular mechanisms of muscle fatigue. Physiol Rev 74: 49–94

Fontaine B, Vale-Santos J, Jurkat-Rott K, Reboul J, Plassart E, Rime CS, Elbaz A, Heine R, Guimaraes J, Weissenbach J et al (1994) Mapping of the hypokalaemic periodic paralysis (HypoPP) locus to chromosome 1q31-32 in three European families. Nat Genet 6:267–272

Graham FL, Rudy J, Brinkley P (1989) Infectious circular DNA of human adenovirus type 5: regeneration of viral DNA termini from molecules lacking terminal sequences. EMBO J 8:2077–2085

Hamill OP, Marty A, Neher E, Sakmann B, Sigworth FJ (1981) Improved patch-clamp techniques for high-resolution current recording from cells and cell-free membrane patches. Pflugers Arch 391:85–100

Hibino H, Inanobe A, Furutani K, Murakami S, Findlay I, Kurachi Y (2010) Inwardly rectifying potassium channels: their structure, function, and physiological roles. Physiol Rev 90:291–366

Inagaki N, Tsuura Y, Namba N, Masuda K, Gonoi T, Horie M, Seino Y, Mizuta M, Seino S (1995) Cloning and functional characterization of a novel ATP-sensitive potassium channel ubiquitously expressed in rat tissues, including pancreatic islets, pituitary, skeletal muscle, and heart. J Biol Chem 270:5691–5694

Kokunai Y, Nakata T, Furuta M, Sakata S, Kimura H, Aiba T, Yoshinaga M, Osaki Y, Nakamori M, Itoh H, Sato T, Kubota T, Kadota K, Shindo K, Mochizuki H, Shimizu W, Horie M, Okamura Y, Ohno K, Takahashi MP (2014) A Kir3.4 Mutation causes Andersen-Tawil syndrome by an inhibitory effect on Kir2.1. Neurology 82:1058–1064

Kristensen M, Hansen T, Juel C (2006) Membrane proteins involved in potassium shifts during muscle activity and fatigue. Am J Physiol 290:R766–R772

Lesage F, Fink M, Barhanin J, Lazdunski M, Mattei MG (1995) Assignment of human G-protein-coupled inward rectifier K+ channel homolog GIRK3 gene to chromosome 1q21-q23. Genomics 29: 808–809

Lim BC, Kim GB, Bae EJ, Noh CI, Hwang H, Kim KJ, Hwang YS, Ko TS, Chae JH (2010) Andersen cardiodysrhythmic periodic paralysis with KCNJ2 mutations: a novel mutation in the pore selectivity filter residue. J Child Neurol 25:490–493

Lopatin AN, Nichols CG (2001) Inward rectifiers in the heart: an update on I(K1). J Mol Cell Cardiol 33:625–638

Ma D, Taneja TK, Hagen BM, Kim BY, Ortega B, Lederer WJ, Welling PA (2011) Golgi export of the Kir2.1 Channel is driven by a trafficking signal located within its tertiary structure. Cell 145:1102–1115

Miake J, Marban E, Nuss HB (2003) Functional role of inward rectifier current in heart probed by Kir2.1 Overexpression and dominant-negative suppression. J Clin Invest 111:1529–1536

Movsesian MA, Schwinger RH (1998) Calcium sequestration by the sarcoplasmic reticulum in heart failure. Cardiovasc Res 37:352–359

Plaster NM, Tawil R, Tristani-Firouzi M, Canun S, Bendahhou S, Tsunoda A, Donaldson MR, Iannaccone ST, Brunt E, Barohn R, Clark J, Deymeer F, George AL Jr, Fish FA, Hahn A, Nitu A, Ozdemir C, Serdaroglu P, Subramony SH, Wolfe G, Fu YH, Ptacek LJ (2001) Mutations in Kir2.1 Cause the developmental and episodic electrical phenotypes of Andersen's syndrome. Cell 105:511–519

Priori SG, Pandit SV, Rivolta I, Berenfeld O, Ronchetti E, Dhamoon A, Napolitano C, Anumonwo J, di Barletta MR, Gudapakkam S, Bosi G, Stramba-Badiale M, Jalife J (2005) A novel form of short QT syndrome (SQT3) is caused by a mutation in the KCNJ2 gene. Circ Res 96:800–807

Raab-Graham KF, Radeke CM, Vandenberg CA (1994) Molecular cloning and expression of a human heart inward rectifier potassium channel. Neuroreport 5:2501–2505

Reiken S, Lacampagne A, Zhou H, Kherani A, Lehnart SE, Ward C, Huang F, Gaburjakova M, Gaburjakova J, Rosemblit N, Warren MS, He KL, Yi GH, Wang J, Burkhoff D, Vassort G, Marks AR (2003) PKA phosphorylation activates the calcium release channel (ryanodine receptor) in skeletal muscle: defective regulation in heart failure. J Cell Biol 160:919–928

Ryan DP, da Silva MR, Soong TW, Fontaine B, Donaldson MR, Kung AW, Jongjaroenprasert W, Liang MC, Khoo DH, Cheah JS, Ho SC, Bernstein HS, Maciel RM, Brown RH Jr, Ptacek LJ (2010) Mutations in potassium channel Kir2.6 Cause susceptibility to thyrotoxic hypokalemic periodic paralysis. Cell 140:88–98

Sacco S, Giuliano S, Sacconi S, Desnuelle C, Barhanin J, Amri EZ, Bendahhou S (2014) The inward rectifier potassium channel Kir2.1 is required for osteoblastogenesis. Hum Mol Genet 24:471–479

Sacconi S, Simkin D, Arrighi N, Chapon F, Larroque MM, Vicart S, Sternberg D, Fontaine B, Barhanin J, Desnuelle C, Bendahhou S (2009) Mechanisms underlying Andersen's syndrome pathology in skeletal muscle are revealed in human myotubes. Am J Physiol 297: C876–C885

Sakura H, Ammala C, Smith PA, Gribble FM, Ashcroft FM (1995a) Cloning and functional expression of the cDNA encoding a novel ATP-sensitive potassium channel subunit expressed in pancreatic beta-cells, brain, heart and skeletal muscle. FEBS Lett 377:338-344

Sakura H, Bond C, Warren-Perry M, Horsley S, Kearney L, Tucker S, Adelman J, Turner R, Ashcroft FM (1995b) Characterization and variation of a human inwardly-rectifying-K-channel gene (KCNJ6): a putative ATP-sensitive K-channel subunit. FEBS Lett 367:193-197

Sejersted OM, Sjogaard G (2000) Dynamics and consequences of potassium shifts in skeletal muscle and heart during exercise. Physiol Rev 80:1411–1481

Standen NB, Stanfield PR (1978) A potential- and time-dependent blockade of inward rectification in frog skeletal muscle fibres by barium and strontium ions. J Physiol 280:169–191

Stoffel M, Espinosa R 3rd, Powell KL, Philipson LH, Le Beau MM, Bell GI (1994) Human G-protein-coupled inwardly rectifying potassium channel (GIRK1) gene (KCNJ3): localization to chromosome 2 and identification of a simple tandem repeat polymorphism. Genomics 21:254–256

Tan SV, Z'Graggen WJ, Boerio D, Rayan DL, Howard R, Hanna MG, Bostock H (2012) Membrane dysfunction in Andersen-Tawil syndrome assessed by velocity recovery cycles. Muscle Nerve 46:193–203

Tristani-Firouzi M, Jensen JL, Donaldson MR, Sansone V, Meola G, Hahn A, Bendahhou S, Kwiecinski H, Fidzianska A, Plaster N, Fu YH, Ptacek LJ, Tawil R (2002) Functional and clinical characterization of KCNJ2 mutations associated with LQT7 (Andersen syndrome). J Clin Invest 110:381–388

Tucker SJ, James MR, Adelman JP (1995) Assignment of KATP-1, the cardiac ATP-sensitive potassium channel gene (KCNJ5), to human chromosome 11q24. Genomics 28:127–128

Vaidyanathan R, Taffet SM, Vikstrom KL, Anumonwo JM (2010) Regulation of cardiac inward rectifier potassium current (I(K1)) by synapse-associated protein-97. J Biol Chem 285: 28000–28009

Ward CW, Reiken S, Marks AR, Marty I, Vassort G, Lacampagne A (2003) Defects in ryanodine receptor calcium release in skeletal muscle from post-myocardial infarct rats. FASEB J 17:1517–1519

Yamada T, Mishima T, Sakamoto M, Sugiyama M, Matsunaga S, Wada M (2006) Oxidation of myosin heavy chain and reduction in force production in hyperthyroid rat soleus. J Appl Physiol (1985) 100: 1520–1526

Yang J, Jan YN, Jan LY (1995) Determination of the subunit stoichiometry of an inwardly rectifying potassium channel. Neuron 15:1441–1447

Yano H, Philipson LH, Kugler JL, Tokuyama Y, Davis EM, Le Beau MM, Nelson DJ, Bell GI, Takeda J (1994) Alternative splicing of human inwardly rectifying K+ channel ROMK1 mRNA. Mol Pharmacol 45:854–860

Yoon G, Quitania L, Kramer JH, Fu YH, Miller BL, Ptacek LJ (2006) Andersen-Tawil syndrome: definition of a neurocognitive phenotype. Neurology 66:1703–1710